HHS Public Access

Author manuscript

J Endod. Author manuscript; available in PMC 2017 January 05.

Published in final edited form as:

J Endod. 2015 February ; 41(2): 225–230. doi:10.1016/j.joen.2014.09.025.

Radiopacifier Particle Size Impacts the Physical Properties of Tricalcium Silicate–based Cements

Mohammad Ali Saghiri, BSc, MSc, PhD[*,†], **James L. Gutmann, DDS, PhD, FACD, FICD, FADI**[‡], **Jafar Orangi, BSc, MSc**[§], **Armen Asatourian, DDS**[§], and **Nader Sheibani, BSc, MSc, PhD**[*,†]

[*]Department of Ophthalmology and Visual Sciences, University of Wisconsin School of Medicine and Public Health, Madison, Wisconsin

[†]Department of Biomedical Engineering, University of Wisconsin School of Medicine and Public Health, Madison, Wisconsin

[‡]Department of Restorative Sciences, Texas A&M University Baylor College of Dentistry, Dallas, Texas

[§]Department of Dental Materials, Kamal Asgar Research Center, Tehran, Iran

Abstract

Introduction—The aim of this study was to evaluate the impact of radiopaque additive, bismuth oxide, particle size on the physical properties, and radiopacity of tricalcium silicate–based cements.

Methods—Six types of tricalcium silicate cement (CSC) including CSC without bismuth oxide, CSC + 10% (wt%) regular bismuth oxide (particle size 10 μm), CSC + 20% regular bismuth oxide (simulating white mineral trioxide aggregate [WMTA]) as a control, CSC + 10% nano bismuth oxide (particle size 50–80 nm), CSC + 20% nano-size bismuth oxide, and nano WMTA (a nano modification of WMTA comprising nanoparticles in the range of 40–100 nm) were prepared. Twenty-four samples from each group were divided into 4 groups and subjected to push-out, surface microhardness, radiopacity, and compressive strength tests. Data were analyzed by 1-way analysis of variance with the post hoc Tukey test.

Results—The push-out and compressive strength of CSC without bismuth oxide and CSC with 10% and 20% nano bismuth oxide were significantly higher than CSC with 10% or 20% regular bismuth oxide ($P < .05$). The surface micro-hardness of CSC without bismuth oxide and CSC with 10% regular bismuth oxide had the lowest values ($P < .05$). The lowest radiopacity values were seen in CSC without bismuth oxide and CSC with 10% nano bismuth oxide ($P < .05$). Nano WMTA samples showed the highest values for all tested properties ($P < .05$) except for radiopacity.

Address requests for reprints to Dr Mohammad Ali Saghiri, Department of Ophthalmology and Visual Sciences, University of Wisconsin School of Medicine and Public Health, 1111 Highland Avenue, 9418 WIMR, Madison, WI 53705. saghiri@gmail.com.

The authors deny any conflicts of interest related to this study.

Conclusions—The addition of 20% nano bismuth oxide enhanced the physical properties of CSC without any significant changes in radiopacity. Regular particle-size bismuth oxide reduced the physical properties of CSC material for tested parameters.

Keywords

Bismuth oxide; compressive strength; nano particle size; radiopacifier; surface hardness

Tricalcium silicate–based cements including mineral trioxide aggregate (MTA) are hydraulic cements composed primarily of tricalcium silicate, dicalcium silicate, and tricalcium aluminate (1, 2). Despite proper physical/chemical properties (3–5), MTA, because of its wide clinical application in pulp capping, root perforation repair, and root-end filling, should possess sufficient radiopacity to allow for distinction from the adjacent anatomic structures such as bone and tooth (6). Tricalcium silicate cements (CSCs) without a radiopacifier have intrinsic radiopacity values ranging from 0.86–2.02 mm aluminum (Al) (7, 8), whereas according to the international standards for dental root canal sealing materials ISO 6876, values lower than 3 mm Al are not recommended (9). Hence, a radiopacifier has to be added to tricalcium silicate–based materials (6).

Bismuth oxide is a radiopacifier agent added to MTA in a 1:4 (wt%) ratio, which provides a radiopacity higher than 3 mm Al as suggested by ISO 6876 (9). ProRoot White MTA (WMTA) (Dentsply Tulsa Dental Specialties, Tulsa, OK) has been reported to have a radiopacity ranging from 5.34–6.92 mm Al (7, 10, 11). Investigators have reported that bismuth oxide is chemically inert in Portland cement (12) or an unreacted filler in hydrated MTA, which is not expected to be significantly incorporated within the hydration structures (13). However, previous authors indicated that physical properties of CSCs, especially compressive strength in a concentration-related manner, could be influenced by the addition of bismuth oxide (13–15).

Nanomodified WMTA is composed of nanoparticles ranging from 40–100 nm $2CaO.SiO_2$, $3CaO.SiO_2$, $3CaO.Al_2O_3$, Bi_2O_3, gypsum, strontium carbonate ($SrCO_3$), zeolite, calcium sulfate ($CaSO_4$), and disodium hydrogen phosphate (Na_2HPO_4) (16, 17). Nano WMTA showed significant improvements in the physiochemical properties of CSCs such as setting time, microhardness (17), push-out bond strength (18, 19), compressive strength (20), osseous reaction (21), and resistance in acidic environments (22).

The impact of the radiopacifier particle size on different properties of CSCs has not been previously investigated. The present study evaluated the effect of particle size and different percentages of bismuth oxide on push-out strength, surface microhardness, radiopacity, and compressive strength of CSCs. We hypothesized that by reducing the particle size of bismuth oxide within the composition of CSCs, such as WMTA, the physical properties will be enhanced without any negative effects on radiopacity of the material.

Materials and Methods

Six types of CSCs were prepared for these studies:

1. CSC without any bismuth oxide

2. CSC with 10% (wt%) regular-size bismuth oxide
3. CSC with 20% (wt%) regular-size bismuth oxide, which was to simulate the WMTA (tooth-colored formula, ProRoot MTA) and served as the control group
4. CSC with 10% (wt%) nano-size bismuth oxide
5. CSC with 20 % (wt%) nano-size bismuth oxide
6. Nano WMTA (US Patent # 8,668,770 B2)

All CSCs were WMTA manufactured by Dentsply (tooth-colored formula, ProRoot MTA) with the same composition except for bismuth oxide. The first CSC was manufactured without bismuth oxide. The second and third group contained 10% (wt%) and 20% (wt%) bismuth oxide with a particle size of 10 μm (Lot: MKBQ9942VP, CAS Number: 1304-76-3; ReagentPlus, Sigma-Aldrich, St Louis, MO), respectively. The fourth and fifth CSC groups were similar to the first CSC group, but 10% (wt%) and 20% (wt%) manually prepared nanosize bismuth oxide was added to the cement base, respectively. Cement powder with a radiopacifier agent was mixed mechanically for 30 seconds at 4500 rpm using an amalgamator (GC America Inc, Alsip, IL). Scanning electron microscope elemental distribution maps (color line and dot maps) were used to confirm the dispersion of bismuth over the CSC + 10% (wt%) nano bismuth oxide powder (Fig. 1*A–C*) (17, 23).

Nano-size bismuth oxide was prepared according to Anilkumar et al (24). Briefly, a known quantity of $Bi(NO_3)$-$5H_2O$ was dissolved in nitric acid, mixed with citric acid in a 1:1 molar ratio, and heated in a water bath. The initial formed gel was decomposed in air to produce a foamy precursor containing uniform flakes of nano-size bismuth oxide. Transmission electron microscopic analysis confirmed the particle size ranged between 50 and 80 nm (Fig. 2*D*).

Push-out Strength

This part was similar to Saghiri et al (18). Briefly, 36 extracted single-rooted human teeth were sectioned horizontally by using a low-speed Isomet diamond saw (Buehler, Lake Bluff, IL) at the midroot part to prepare dentin slices with 2-mm thickness. The canal spaces were instrumented by using #2 through #5 Gates-Glidden burs (Mani, Tochigi, Japan) to form 1.3-mm-diameter standardized spaces. Subsequently, debris and smear layer removal was done by immersion in 17% EDTA followed by 5.25 % sodium hypochlorite for 1 minute in each solution.

According to the filling material, the specimens were divided into 6 groups of 6 ($n = 6$), and mentioned cements were mixed according to the manufacturers' instructions (a water to cement ratio of 1:3) and transferred into the canal spaces using a manual MTA carrier and packed by using a hand compactor. A piece of gauze soaked in synthetic tissue fluid was placed on each sample before incubation at 37°C and 98% humidity for 3 days.

The Z050 (Zwick/Roell, Ulm, Germany) universal testing machine was used to measure the push-out strength. Samples were fixed on a metal slab with a central hole, and a stainless steel plunger with a 1-mm diameter was used to apply the downward compressive load with

a crosshead speed of 1 mm/min on the cement materials. To ensure that the contact is only between the plunger and CSCs, a clearance of approximately 0.2 mm from the margin of the dentinal wall was embedded.

Surface Microhardness

According to Saghiri et al (25), 36 glass tubes were divided into 6 experimental groups similar to the first part of study. Cements were mixed and packed into the plastic tubes, and after incubation for 24 hours, they were grounded and prepared for the Vickers hardness test. At room temperature, a full load of 50 g was applied to the cement surface for 5 seconds. The procedure was repeated 3 times, and the mean value of the hardness was recorded as the hardness value for each specimen.

Evaluation of Radiopacity

This part was determined according to the methods prescribed by the ISO 6876:2012 for dental root canal sealing materials and similar to Camilleri and Gandolfi (26). Briefly, 6 samples from each 1 of 6 cement types were mixed with water and allowed to set for 24 hours at 37°C and 98% relative humidity. Samples were stored in distilled water at 37°C for 7 days after removal from the molds.

An occlusal X-ray film (Kodak Insight, Rochester, NY) along with an aluminum (99.5% pure) step wedge with step heights ranging from 1–10 mm in increments of 1 mm were placed directly under the specimens. The target to film distance was set as a fix parameter at 100 cm. A standard X-ray machine (General Electric Company, Milwaukee, WI) at a tube voltage of 50 kV and an exposure time of 0.05 seconds was used to irradiate the X-ray.

The base and fog value, deducted from the gross radiographic density, was used to calculate the net radiographic density. For each radiograph, the net radiographic density of the aluminum steps (NRD_{Al}) versus the logarithm of the thickness of aluminum (log d) was plotted. The gradient and the intercept were calculated from the resultant plots. The following formula was used to obtain linear regression of the data:

$$\mathrm{NRD}_{Al} = \mathrm{m.logd} + \mathrm{I}$$

where m and I were the gradient and the intercept, respectively.

Compressive Strength

This test was performed in accordance with ISO 9917-1:2007 standards and was similar to Saghiri et al. (20). Briefly, 6 samples of each cement type (overall 36 specimens) were mixed and placed inside 36 one-end closed split stainless steel molds with 6-mm width and 9-mm height and incubated for 3 days at a constant temperature of 37°C and 98% humidity. Specimens were removed from the molds and placed lengthwise between the platens of an Instron 85215 (Instron Corp, Canton, MA) testing machine. Before removing the samples from the molds, they were probed with an explorer to identify solidity. A compression rate of 1 mm/min was applied, and the load at fracture (MPa) was recorded. The following formula was used to calculate the compressive strength:

$$\text{Compressive strength} = \left[(\text{failure load})/(\text{width of plug}/2)^2 * \pi\right]$$

Statistical Analysis

Data were analyzed by 1-way analysis of variance and post hoc Tukey tests. The level of significance was considered as $P < .05$.

Results

Push-out Strength

Nano WMTA and CSC with 10% regular bismuth oxide showed the highest and lowest values, respectively. The average push-out strengths varied from 89.4 ± 7.3 to 138.7 ± 7.4 MPa among the groups (Fig. 3*A*). CSC without bismuth oxide showed significantly higher push-out strength than CSC with 10% and 20% regular- and 10% nano-size bismuth oxide ($P < .05$). This difference was not significant when compared with CSC with 20% nano bismuth oxide ($P > .05$). The CSC with 10% and 20% regular-size bismuth oxide were similar to each other ($P > .05$) and showed significantly lower push-out strength than all cement types ($P < .05$). The push-out strength of CSC with 10% and 20% nano bismuth oxide were also not significantly different from each other ($P = .572$), whereas they were significantly higher than all other cement types ($P < .05$), except for nano WMTA.

Surface Microhardness

The average surface microhardness varied from 40.1 ± 3.5 to 91.4 ± 4.8 MPa among the groups (Fig. 3*B*). Nano WMTA showed the highest, and CSC with 10% regular bismuth oxide showed the lowest values among other groups ($P < .05$). Surface microhardness of CSC without bismuth oxide was only higher than CSC with 10% regular bismuth oxide ($P < .05$), whereas it was significantly lower than all other cement types ($P < .05$). The surface microhardness values of CSC with 20% regular bismuth oxide (WMTA) and CSC with 10% nano bismuth oxide were similar ($P = 1.00$) and significantly higher than CSC without and with 10% regular bismuth oxide ($P < .05$) and significantly lower than CSC with 20% nano bismuth oxide and nano WMTA ($P < .001$). The surface microhardness value of CSC with 20% nano bismuth oxide was significantly higher than all cement types ($P < .001$), whereas it was lower than nano WMTA ($P = .039$).

Evaluation of Radiopacity

The radiopacity of CSC without bismuth oxide was the lowest value ($P < .001$), and the CSC with 20% regular-size bismuth oxide (WMTA) showed the highest value of radiopacity among all groups. The radiopacity values of CSC without and with 10% nano bismuth oxide were significantly lower than other cement types ($P < .001$), whereas among other groups significant differences were not detected ($P > .05$). The radiopacity varied from 1.9 ± 0.3 to 8.8 ± 0.5 mm of equivalent Al for these samples (Fig. 3*C*).

Compressive Strength

The highest and lowest values were seen in nano WMTA and CSC with 20% regular-size bismuth oxide (WMTA). The compressive strength values of CSC with 10% and 20% regular bismuth oxide were similar ($P = .054$) and significantly lower than all other cements ($P < .001$). The CSC with 10% and 20% nano bismuth oxide showed similar compressive strength values ($P = .974$), which were significantly higher than all other cements ($P < .001$) but lower than the nano WMTA value ($P < .05$). The average compressive strengths varied from 45.3 ± 2.8 to 128.1 ± 12.3 MPa among the groups (Fig. 3*D*).

Discussion

The microstructure of hydrated MTA would likely be weaker when compared with that of Portland cement (13). This is mainly attributed to differences in their composition such as bismuth oxide particles. Bismuth oxide is confirmed to act as an inert additive, which does not contribute to the hydration reactions (13, 27). Previous studies showed that bismuth oxide particles can negatively affect compressive strength of cements (13–15). Therefore, this study sought to understand the effect of bismuth oxide particle size with different percentages on a wide range of physical properties including pushout strength, surface microhardness, compressive strength, and radiopacity of MTA-like cements.

Because data regarding the bismuth oxide particle size used in ProRoot MTA were not available, in the current study CSCs without bismuth oxide were ordered to unify the bismuth oxide characteristics including particle size used in experimental groups. Bismuth oxide with 2 particle sizes (10 μm) and (50–80 nm) were mixed with CSCs in 20% (wt%) to simulate ProRoot MTA and nano WMTA cements, respectively. The results showed that nano WMTA had favorable physical properties compared with CSCs with 20% (wt%). Nano bismuth oxide that might contribute to the ingredients was added to nano WMTA as mentioned previously. The nano WMTA–measured physical properties were consistent with measurements from previous studies (16–19, 21, 27, 28).

The hydration of CSC begins with the formation of cubic and needlelike crystals (ettringite) in an interlocking orientation in cement structure (21–24). The bismuth oxide particles can affect the hydration process of MTA by their distribution inside the hydrated cement material (2). Hence, the nano-size bismuth oxide particles, because of their higher surface area, can affect the hydrated structure of cement in a way that the orientation of ettringite crystals can become more uniform, resulting in a dense and solid cement structure (29). This outcome supports the findings in the present study that nano bismuth oxide enhanced the physical properties of the tested cements.

The push-out test assesses the integrity of a material with its surrounding root canal dentin (18, 30, 31). Our results indicated that CSC without bismuth oxide had significantly higher push-out strength and compression strength than CSC with 10% and 20% regular bismuth oxide. These results are consistent with findings of previous authors (13–15, 18). We found that the compressive strength was reduced in a concentration-dependent manner when regular bismuth oxide was added to the MTA-like cement. However, nano-bismuth oxide significantly increased the compressive strength of CSC materials. These findings might be

explained by the increased surface area of bismuth oxide particles, which caused an increase in the formation of ettringite crystals. However, the more uniform distribution of nano bismuth particles may result in better orientation of ettringite crystals providing a better interlocking mass in cement structure (Fig. 2*A–C*).

Microhardness and porosity have an inverse relationship (32, 33). The addition of bismuth oxide had a favorable effect on the microhardness of CSCs, which is consistent with the results of a previous investigation (32). Moreover, the nano form of bismuth oxide had more impact than its regular form, which might be attributed to the smaller porosity of the nano form compared with the regular form (32). The nano powder reinforces the cement by filling the very small areas between hydration products and also enhances the orientation and precipitation of ettringite needles as shown schematically in Figure 2*B*. The greater porosity might accelerate crack propagation into the surface texture and decrease the surface microhardness.

All experimental groups except CSC without bismuth oxide showed radiopacity values greater than 3-mm thickness of Al. This implies that all mixtures can be candidates for root-end filling materials in terms of their radiopacity. However, CSC with 10% nano bismuth oxide showed lower values, which might be caused by the lower percentage of bismuth oxide. The CSC with 20% nano bismuth oxide mixture did not show significant differences in radiopacity when compared with groups containing regular bismuth oxide. Nano-form materials might have a relatively lower radiopacity to X-rays, and they have the potential to be agglomerated. Nano WMTA showed significantly higher radiopacity among nano mixture experimental groups and almost equal radiopacity with the CSC with 20% regular bismuth oxide (WMTA) group. The excessive amount of ($3CaO.Al_2O_3$) in the composition of nano WMTA may justify this increase.

Nano WMTA showed the highest physical property values compared with other groups. This issue might be explained by its higher surface area and excessive amount of ettringite phase as shown in Figure 2*C*. Furthermore, nano-size powder will better accommodate and fill small gap spaces, which might result in an increase of the mechanical properties of cement. Nano WMTA also consists of elements such as strontium salt and carbonate and zeolite, which are stabilizer agents (16, 17). Furthermore, scanning electron microscopic analysis of strontium aluminate in combination with gypsum showed that this component can reduce the size of ettringite, which in turn could decrease the void size between ettringite needlelike crystals (34). These findings are also consistent with previously published investigations (18, 20).

Conclusion

We found the following:

1. Bismuth oxide impacted all tested physical properties. The addition of regular-size bismuth oxide decreased, whereas the nano-size particles enhanced the physical properties of CSC.

2. The optimum percentage for the addition of nano-size bismuth oxide was at least 20% (wt%) to achieve a material with enhanced physical properties and acceptable radiopacity.

3. Reducing the size of all particles to a nano level, as seen in nano WMTA, produced a more homogenous cement with outstanding physical characteristics.

Acknowledgments

The authors thank ProRoot WMTA manufacturing company (Dentsply Tulsa Dental Specialties, Tulsa, OK) for providing us with required cement materials for this study.

Also special thanks to Dr Mehrdad Lotfi for all his contributions to this research.

Mohammad Ali Saghiri holds a U.S. patent for Nano Cement (US 8,668,770 B2).

References

1. Camilleri J, Montesin FE, Brady K, et al. The constitution of mineral trioxide aggregate. Dent Mater. 2005; 21:297–303. [PubMed: 15766576]
2. Camilleri J. Characterization of hydration products of mineral trioxide aggregate. Int Endod J. 2008; 41:408–17. [PubMed: 18298574]
3. Saghiri MA, Lotfi M, Saghiri AM, et al. Effect of pH on sealing ability of white mineral trioxide aggregate as a root-end filling material. J Endod. 2008; 34:1226–9. [PubMed: 18793926]
4. Vosoughhosseini S, Lotfi M, Shahi S, et al. Influence of white versus gray mineral trioxide aggregate on inflammatory cells. J Endod. 2008; 34:715–7. [PubMed: 18498897]
5. Saghiri MA, Asgar K, Daliri M, et al. Morphological behavior and attachment of p19 neural cells to root-end filling materials. Scanning. 2010; 32:369–74. [PubMed: 21254110]
6. Beyer-Olsen EM, Ørstavik D. Radiopacity of root canal sealers. Oral Surg Oral Med Oral Pathol. 1981; 51:320–8. [PubMed: 6938892]
7. Islam I, Kheng Chng H, Jin Yap AU. Comparison of the physical and mechanical properties of MTA and Portland cement. J Endod. 2006; 32:193–7. [PubMed: 16500224]
8. Saliba E, Abbassi-Ghadi S, Vowles R, et al. Evaluation of the strength and radiopacity of Portland cement with varying additions of bismuth oxide. Int Endod J. 2009; 42:322–8. [PubMed: 19220518]
9. International Standards Organization. Dental Root Canal Sealing Materials BS EN ISO 6876-7.8. 2002
10. Kim E-C, Lee B-C, Chang H-S, et al. Evaluation of the radiopacity and cytotoxicity of Portland cements containing bismuth oxide. Oral Surg Oral Med Oral Pathol Oral Radiol Endod. 2008; 105:e54–7. [PubMed: 18155604]
11. Danesh G, Dammaschke T, Gerth H, et al. A comparative study of selected properties of ProRoot mineral trioxide aggregate and two Portland cements. Int Endod J. 2006; 39:213–9. [PubMed: 16507075]
12. Leonard NM, Wieland LC, Mohan RS. Applications of bismuth (III) compounds in organic synthesis. Tetrahedron. 2002; 58:8373–97.
13. Camilleri J. Hydration mechanisms of mineral trioxide aggregate. Int Endod J. 2007; 40:462–70. [PubMed: 17459120]
14. Coomaraswamy KS, Lumley PJ, Hofmann MP. Effect of bismuth oxide radioopacifier content on the material properties of an endodontic Portland cement–based (MTA-like) system. J Endod. 2007; 33:295–8. [PubMed: 17320718]
15. Camilleri J. The physical properties of accelerated Portland cement for endodontic use. Int Endod J. 2008; 41:151–7. [PubMed: 17931386]

16. Saghiri, MA.; Lotfi, M.; Aghili, H. Dental cement composition. United States: InventorsU.S. patent. US 8,668,770 B2, United States. Available at: http://www.google.com/patents/US8668770. Accessed November 4, 2014
17. Saghiri MA, Asgar K, Lotfi M, Garcia-Godoy F. Nanomodification of mineral trioxide aggregate for enhanced physiochemical properties. Int Endod J. 2012; 45:979–88. [PubMed: 22519859]
18. Saghiri MA, Garcia-Godoy F, Gutmann JL, et al. Push-out bond strength of a nano-modified mineral trioxide aggregate. Dent Traumatol. 2013; 29:323–7. [PubMed: 22882995]
19. Saghiri, MA.; Asatourian, A.; Garcia-Godoy, F., et al. The impact of thermocycling process on the dislodgement force of different endodontic cements; Biomed Res Int. 2013. p. 2013Article ID 317185. Available at: http://dx.doi.org/10.1155/2013/317185. Accessed November 4, 2014
20. Saghiri MA, Garcia-Godoy F, Asatourian A, et al. Effect of pH on compressive strength of some modification of mineral trioxide aggregate. Med Oral Patol Oral Cir Bucal. 2013; 18:e714–20. [PubMed: 23722137]
21. Saghiri MA, Orangi J, Tanideh N, et al. Effect of endodontic cement on bone mineral density using serial dual-energy X-ray absorptiometry. J Endod. 2014; 40:648–51. [PubMed: 24767558]
22. Saghiri MA, Garcia-Godoy F, Gutmann JL, et al. The effect of pH on solubility of nano-modified endodontic cements. J Conserv Dent. 2014; 17:13–7. [PubMed: 24554853]
23. Saghiri MA, Asgar K, Lotfi M, et al. Back-scattered and secondary electron images of scanning electron microscopy in dentistry: a new method for surface analysis. Acta Odontol Scand. 2012; 70:603–9. [PubMed: 22251068]
24. Anilkumar M, Pasricha R, Ravi V. Synthesis of bismuth oxide nanoparticles by citrate gel method. Ceram Int. 2005; 31:889–91.
25. Saghiri M, Lotfi M, Saghiri A, et al. Scanning electron micrograph and surface hardness of mineral trioxide aggregate in the presence of alkaline pH. J Endod. 2009; 35:706–10. [PubMed: 19410088]
26. Camilleri J, Gandolfi M. Evaluation of the radiopacity of calcium silicate cements containing different radiopacifiers. Int Endod J. 2010; 43:21–30. [PubMed: 19891720]
27. Li Q, Coleman NJ. Early hydration of white Portland cement in the presence of bismuth oxide. Adv Appl Ceram. 2013; 112:207–12.
28. Saghiri MA, Nazari A, Garcia-Godoy F, et al. Mechanical response of dental cements as determined by nanoindentation and scanning electron microscopy. Microsc Microanal. 2013; 19:1458–64. [PubMed: 24067263]
29. Kurtis, K. Effects of Titanium Dioxide Nanoparticles on Structure and Performance of Cementitious Materials. Pontificia Universidad Catolica de Chile. 2013. Available at: http://reactor.ing.puc.cl/ingenieria-y-gestion-construccion/wp-content/uploads/2013/10/kurtis-student-presentation-tio2-chile.pdf. Accessed October 30, 2014
30. Shahi S, Rahimi S, Yavari HR, et al. Effects of various mixing techniques on push-out bond strengths of white mineral trioxide aggregate. J Endod. 2012; 38:501–4. [PubMed: 22414837]
31. Hong S-T, Bae K-S, Baek S-H, et al. Effects of root canal irrigants on the push-out strength and hydration behavior of accelerated mineral trioxide aggregate in its early setting phase. J Endod. 2010; 36:1995–9. [PubMed: 21092820]
32. Saghiri MA, Lotfi M, Joupari MD, et al. Effects of storage temperature on surface hardness, microstructure, and phase formation of white mineral trioxide aggregate. J Endod. 2010; 36:1414–8. [PubMed: 20647108]
33. Nekoofar M, Adusei G, Sheykhrezae M, et al. The effect of condensation pressure on selected physical properties of mineral trioxide aggregate. Int Endod J. 2007; 40:453–61. [PubMed: 17459121]
34. Velazco G, Almanza J, Cortés D, et al. Effect of the strontium aluminate and hemihydrate contents on the properties of a calcium sulphoaluminate based cement. Mater Construcc. 2014; 64:e0–24.

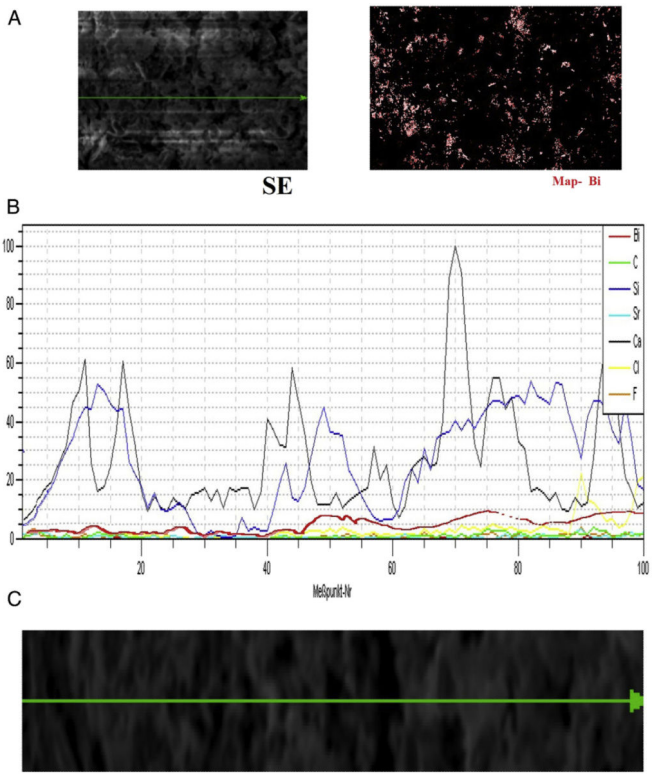

Figure 1.

Scanning electron microscopic (SEM) elemental distribution maps of bismuth over the CSC + 10% (wt%) nano bismuth oxide powder. (*A*) *Left*: SEM secondary electron mode of powder surface (×2000). *Right*: Cement powder bismuth distribution color dot map. (*B*) The elemental distribution plot of CSCs + 10% nano bismuth oxide. (*C*) Line scan direction of elemental distribution. SE, scanning electron microscope.

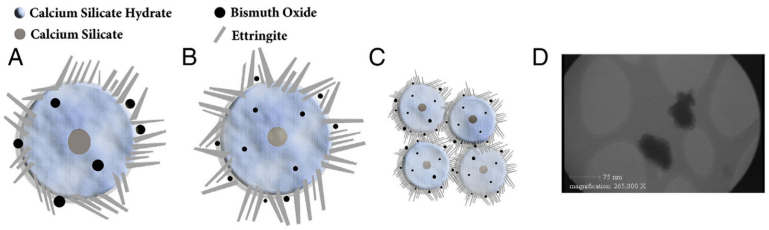

Figure 2.

A schematic figure of the calcium silicate hydrate structure with calcium silicate nucleus, needlelike ettringite crystals, and bismuth oxide particles in 3 types of cements: (*A*) CSC with regular-size bismuth oxide, (*B*) CSC with nano-size bismuth oxide particles, and (*C*) nano WMTA cement with nano-size particles. In *B*, the better distribution of nano bismuth oxide particles between ettringite crystals can be seen, which may result in better interlocking mass formation. Note the orientation of ettringite crystals in *B*, which because of the nano size of bismuth oxide, particles can make better contact and integrity with each other. (*D*) Transmission electron microscopic image of particles that confirmed the range size from 50–80 nm.

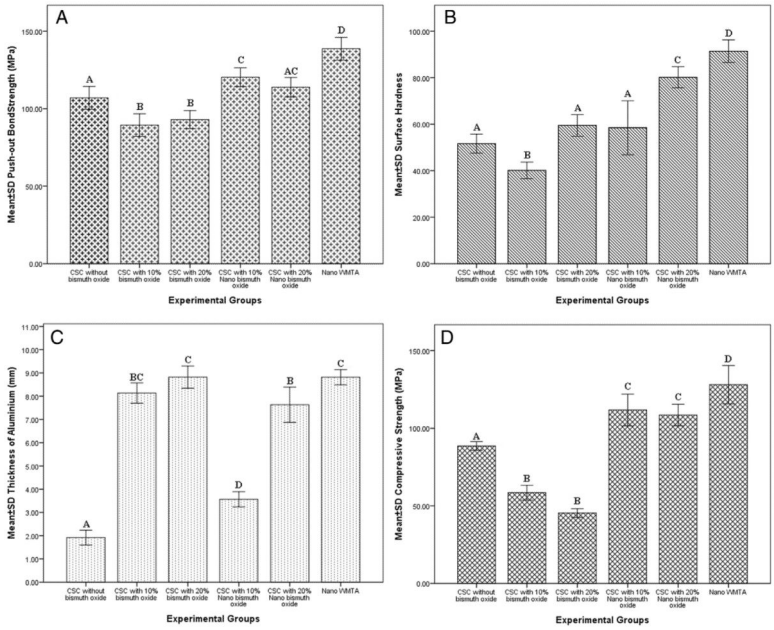

Figure 3.

The comparison of physical property and radiopacity values of experimental groups. (*A*) The push-out strength values. (*B*) The surface microhardness values. (*C*) The radiopacity (thickness of Al slab) values. (*D*) The compressive strength values. The groups with different letters were significantly different.